Proceedings of the 7th GACM Colloquium on Computational Mechanics
for Young Scientists from Academia and Industry
October 11-13, 2017 in Stuttgart, Germany

A primal discontinuous Petrov Galerkin Finite Element Method

Tobias Steiner[1]* and Peter Wriggers[1]

Micro Abstract
In this contribution a primal discontinuous Petrov Galerkin Finite Element Method (dPG FEM) with a linear elastic isotropic material model is presented. This novel mixed discretization method was introduced by Demkowicz and Gopalakrishnan in 2010. The behavior of this formulation is studied with benchmark simulations for small deformations in the nearly incompressible case. Furthermore, a possible extension for a nonlinear Finite Element formulation is suggested.

[1]Institute of Continuum Mechanics, Leibniz Universität Hannover, Hannover, Germany
***Corresponding author**: steiner@ikm.uni-hannover.de

Introduction

In the engineering practice, due to their reliability, standard Galerkin Finite Element Methods are a powerful tool in solid mechanics since decades. Also the mixed finite element technology is popular in linear elasticity for stress approximations and robust for (nearly) incompressible material behaviour as the Poissons ratio ν tends to 0.5 in the limiting case. However, there are still several applications that limit the use of standard finite element schemes. These are related to locking in various forms, like shear or volume locking. In this contribution, we concentrate on the phenomenon indicated as volume locking which can lead to failure of a numerical method when constraints, as related to incompressible material behaviour, are not taken into account properly. The focus of this research topic is on the introduction of a novel discretization method for linear elasticity, which is able to overcome the phenomenon of volume locking. The basis for this is the discontinuous Petrov-Galerkin (dPG) Finite Element Method (FEM) proposed recently by L. Demkowicz and J. Gopalakrishnan in [2,3] for the transport equation and by C. Carstensen et al. in [1] for the Poisson model problem.

Formulation

In this section, we provide the derivation of the weak form of the dPG FEM for linear elasticity. We consider a domain Ω given in Fig. 1 with the governing equations for linear elasto-statics:

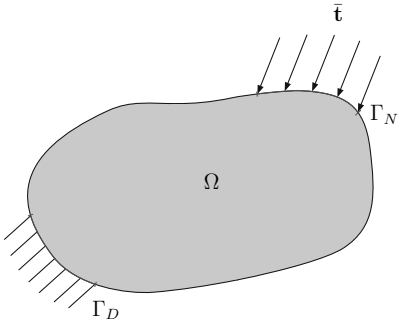

Figure 1. Domain Ω, with Dirichlet boundary Γ_D and Neumann boundary Γ_N.

$$
\begin{aligned}
&\operatorname{div}(\boldsymbol{\sigma}(\boldsymbol{\varepsilon})) + \rho\mathbf{b} = \mathbf{0} && \text{in } \Omega \\
&\boldsymbol{\sigma}\cdot\mathbf{n} = \bar{\mathbf{t}} && \text{on } \Gamma_N \\
&\mathbf{u} = \bar{\mathbf{u}} && \text{on } \Gamma_D \\
&\boldsymbol{\sigma}(\boldsymbol{\varepsilon}) = \boldsymbol{\mathcal{C}} : \boldsymbol{\varepsilon}(\mathbf{u}) && \text{in } \Omega \\
&\boldsymbol{\varepsilon}(\mathbf{u}) = \tfrac{1}{2}(\operatorname{grad}(\mathbf{u}) + \operatorname{grad}^T(\mathbf{u}))
\end{aligned}
\qquad (1)
$$

In Eq. (1), $\boldsymbol{\sigma}$ denotes the stress tensor, ρ the mass density and $\mathbf{b}$ the body forces in the domain Ω. The expression for the static boundary condition, $\boldsymbol{\sigma} \cdot \mathbf{n} = \bar{\mathbf{t}}$, with the normal vector $\mathbf{n}$, is defined on the Neumann boundary Γ_N as the traction vector $\bar{\mathbf{t}}$. Prescribed displacements on the Dirichlet boundary Γ_D are denoted by $\bar{\mathbf{u}}$, and the linear elastic relation between stresses $\boldsymbol{\sigma}(\boldsymbol{\varepsilon})$ and strains $\boldsymbol{\varepsilon}(\mathbf{u})$ are achieved by the isotropic fourth order material tensor $\boldsymbol{\mathcal{C}}$. The general weak form can now be obtained by multiplication of the balance of linear momentum in Eq. $(1)_1$ with a test function $\boldsymbol{\eta}$ and integration by parts on a single triangle T of the triangulation $\mathcal{T}$:

$$\int_T \boldsymbol{\sigma}(\varepsilon) : \operatorname{grad}(\boldsymbol{\eta}) \, \mathrm{d}A - \int_{\partial T} \underbrace{\boldsymbol{\sigma} \cdot \boldsymbol{n}_T}_{=:\mathbf{t_T}} \cdot \boldsymbol{\eta} \, \mathrm{d}s \;=\; \int_T \rho \mathbf{b} \cdot \boldsymbol{\eta} \, \mathrm{d}A. \tag{2}$$

Besides the classical interpolation of element displacements $\mathbf{u}$, the occuring boundary integral ∂T with the tractions $(\boldsymbol{\sigma} \cdot \boldsymbol{n}_T)$ at the interface of adjoined elements is also evaluated. In this context an additional variable $\mathbf{t_T}$ for the tractions is introduced resulting in a mixed formulation with displacements $\mathbf{u}$ and tractions $\mathbf{t_T}$ as primary unknowns. The weak form for the primal discontinuous Petrov-Galerkin FEM can now be obtained by summing up over all triangles T of the triangulation $\mathcal{T}$ and yields

$$\int_\Omega \operatorname{grad}^T_{\mathrm{NC}}(\boldsymbol{\eta}) : \boldsymbol{\mathcal{C}} : \operatorname{grad}(\mathbf{u}) \, \mathrm{d}A - \sum_{T \in \mathcal{T}} \int_{\partial T} \boldsymbol{\eta}^T \cdot \mathbf{t_T} \, \mathrm{d}s \;=\; \int_\Omega \boldsymbol{\eta}^T \cdot \rho \mathbf{b} \, \mathrm{d}A, \tag{3}$$

where $\operatorname{grad}_{\mathrm{NC}}$ denotes the *non-conforming* gradient with which a discontinuity in the space of the test functions is introduced. The second integral in Eq. (3) describes the summation of the contributions from tractions at the edges of all elements in the domain. For further implementation of the dPG FEMs weak form in a finite element framework triangular elements with six nodes, each with two degrees of freedom (dof), are used (cf. Fig. 2). The three corner nodes are related to the displacements $\mathbf{u}$ and the three mid-side nodes refer to the tractions $\mathbf{t_T}$ at the edge. Due to introducing tractions on the interfaces between elements, respect has to be given to the direction of the unit outward normal vector on coinciding edges (see Fig. 2) and a preferred or positive flow direction has to be determined. Afterwards, the discretization of displacements $\mathbf{u}$, tractions $\mathbf{t_T}$ and test functions $\boldsymbol{\eta}$ is introduced to achieve a low-order finite element formulation. Here, standard Lagrangian polynomials for the approximation of the displacements $\mathbf{u}$ and the test functions $\boldsymbol{\eta}$ are used. Furthermore, the interpolation of the tractions $\mathbf{t_T}$ is accomplished with constant functions on the edges. Following, the discretized weak form of the primal dPG FEM in a matrix notation is utilized, which is more convenient than a direct index implementation, and yields

$$\sum_{I=1}^{3} \sum_{J=1}^{3} \hat{\boldsymbol{\eta}}_I^T \left(\int_\Omega \mathbf{B}_I^T \cdot \boldsymbol{\mathcal{C}}_{2D} \cdot \mathbf{B}_J \, \mathrm{d}A \cdot \hat{\mathbf{u}}_J + \sum_{T \in \mathcal{T}} \int_{\partial T} \mathbf{N}_I^T \cdot \hat{\mathbf{N}}_J \, \mathrm{d}s \cdot \hat{\mathbf{t}}_J \right) \;=\; \sum_{I=1}^{3} \hat{\boldsymbol{\eta}}_I^T \int_\Omega \mathbf{N}_I^T \cdot \rho \mathbf{b} \, \mathrm{d}A, \tag{4}$$

where $\mathbf{N}$ contains the linear Lagrangian shape functions over the triangular element, $\hat{\mathbf{N}}$ the constant shape functions on the edges and $\mathbf{B}$ the derivatives of the linear shape functions. With $\hat{\bullet}$ the approximation of the unknowns $\mathbf{u}$ and $\mathbf{t}$, respectively, and the test function $\boldsymbol{\eta}$ is characterized.In order to evaluate the integrals numerically an appropriate Gauss quadrature scheme on the domain Ω as well as on the edge ∂T is applied. This results in a mixed system of equations consisting of two matrices ($\mathbf{A}\,(6 \times 6)$ and $\mathbf{D}\,(6 \times 6)$) from the volume and boundary term (cf. Eq. (5)).

As a consequence, the element stiffness matrix has a non-square shape due to the use of the same test functions for both primary variables:

$$\underbrace{\begin{bmatrix}\mathbf{A} & | & \mathbf{D}\end{bmatrix}}_{\mathbf{G}(6\times 12)} \cdot \begin{bmatrix}\hat{\mathbf{u}} \\ \hat{\mathbf{t}}\end{bmatrix} = \begin{bmatrix}\hat{\mathbf{f}}\end{bmatrix} \tag{5}$$

$$\text{with} \quad \mathbf{A} = \int_{\Omega} \mathbf{B}_I^T \cdot \boldsymbol{\mathcal{C}}_{2D} \cdot \mathbf{B}_J \, \mathrm{d}V, \qquad \mathbf{D} = \int_{\partial T} \mathbf{N}_I^T \cdot \hat{\mathbf{N}}_J \, \mathrm{d}s, \qquad \hat{\mathbf{f}} = \int_{\Omega} \mathbf{N}_I^T \cdot \rho \mathbf{b} \, \mathrm{d}V.$$

Consider two neighbouring triangular finite elements (cf. Fig. 2) whereas each has three nodes for displacements (∘) and three nodes for tractions (⋄) with two degrees of freedom per node, leads to 12 degrees of freedom per element. Furthermore, continuity for displacements $\hat{\mathbf{u}}$ and tractions $\hat{\mathbf{t}}$ is assumed, but due to utilization of discontinuous test functions, assembling is at first only accomplished for the primary variables reducing the amount of degrees of freedom to 18 instead of 24 for decoupled elements. The non-continuity due to the interpolation of the test functions as non-conforming or *broken*, results in test functions which "live" on each element separately. The global system of equations for two adjoined elements then yields a matrix of size $\mathbf{G}\,(12 \times 18)$.

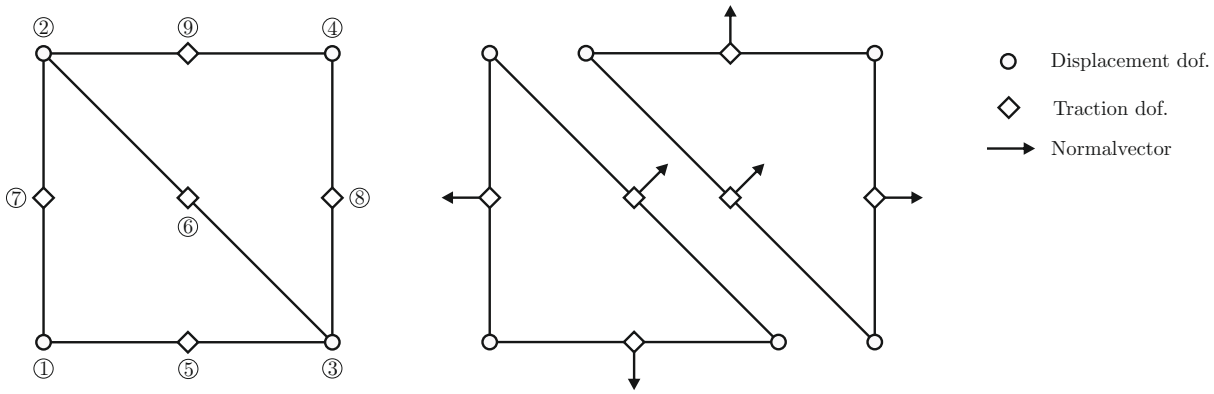

Figure 2. *left:* Global node numbering for displacement degrees of freedom (∘) and traction degrees of freedom (⋄). *right:* description of preferred direction of normal vector on coinciding element interfaces.

A global stiffness matrix of square shape and a right hand side with matching size is obtained by multiplication of the left and right hand side after assembly with the transposed of the non-square linear system of equations $\mathbf{G}^T$. Since $\mathbf{G}^T \cdot \mathbf{G}$ leads to a rank deficiency resulting in a singular matrix, a stabilization matrix $\mathbf{M}$ is introduced in terms of an integral formulation over the domain with the test functions appearing in the weak form:

$$\mathbf{M} = \int_{\Omega} \left(\mathrm{grad}_{\mathrm{NC}}^T(\boldsymbol{\eta}) : \boldsymbol{\mathcal{C}} : \mathrm{grad}_{\mathrm{NC}}(\boldsymbol{\eta}) + \boldsymbol{\eta}^T \cdot \boldsymbol{\eta} \right) \mathrm{d}A. \tag{6}$$

Afterwards, a square shaped and symmetric system of equations is achieved by $\mathbf{G}^T\mathbf{M}^{-1}\mathbf{G} \cdot \hat{\mathbf{x}} = \mathbf{G}^T\mathbf{M}^{-1}\hat{\mathbf{f}}$, with $\hat{\mathbf{x}}$ the vector of unknowns. After introducing Dirichlet and Neumann boundary conditions the system can be directly solved for the unknowns $\hat{\mathbf{u}}$ and $\hat{\mathbf{t}}$.

Results

In this example, the performance of the proposed formulation is tested and compared with classical Galerkin finite elements and mixed finite element formulations for the well-known Cook's Membrane problem.

System setup:

right side:	$\mathbf{t}_T$	=	$(0,1)$ $\left[\mathrm{N/mm^2}\right]$
upper & lower side:	$\mathbf{t}_T$	=	$(0,0)$ $\left[\mathrm{N/mm^2}\right]$
left side:	$\mathbf{u}$	=	$(0,0)$ [mm]
Young's modulus:	E	=	210 $\left[\mathrm{N/mm^2}\right]$
Poisson's ratio:	ν	=	0.499

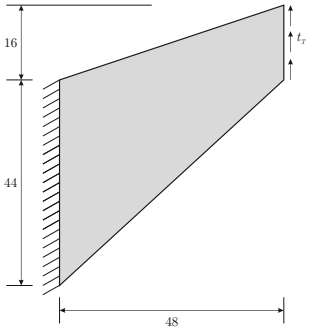

Figure 3. *left:* Material parameters and boundary conditions. *right:* Geometry of Cook's Membrane problem.

In Fig. 4 the convergence of the vertical displacement during mesh refinement is shown for different classical Galerkin formulations (*left*) and mixed formulations (*right*) compared to the proposed mixed T1-dPG formulation. The T1-dPG formulation has a better convergence than elements with linear interpolations (T1 & Q1), but is still insufficient compared to higher-order elements (T2 & Q2) and mixed finite element formulations in the nearly incompressible case.

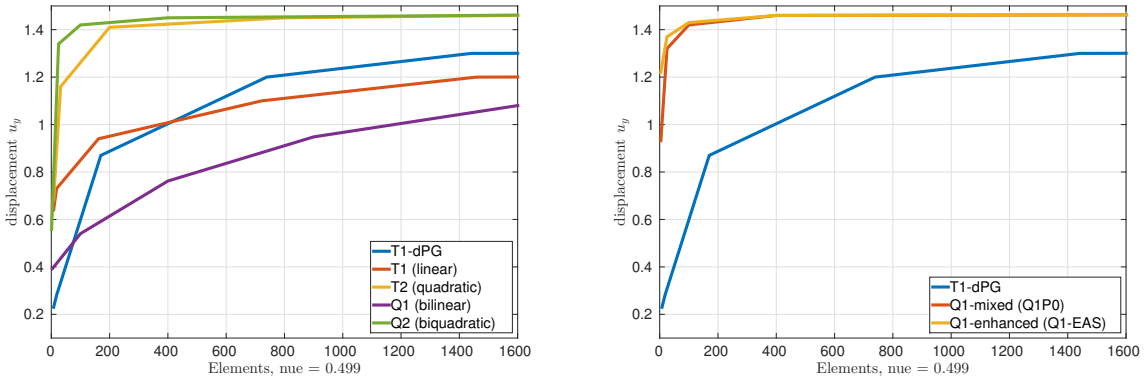

Figure 4. Convergence of vertical displacement of the top right point for the dPG FEM compared to classical Galerkin formulations (*left*) and mixed formulations (*right*).

Outlook

The primal dPG FEM for linear elastic material behaviour will be tested extensively for further benchmark tests and compared with well-known finite element formulations. In a next step, investigations on the extension and implementation of a nonlinear primal discontinuous Petrov-Galerkin Finite Element Method (e.g. St. Venant or Neo-Hookean material) are conducted.

Acknowledgements

The authors gratefully acknowledge the support by the Deutsche Forschungsgemeinschaft in the Priority Program 1748.

References

[1] C. Carstensen, D. Gallistl, F. Hellwig, and L. Weggler. Low-order dpg-fem for an elliptic pde. *Computers & Mathematics with Applications*, 68(11):1503 – 1512, 2014.

[2] L. Demkowicz and J. Gopalakrishnan. A class of discontinuous petrov–galerkin methods. part i: The transport equation. *Computer Methods in Applied Mechanics and Engineering*, 199(23–24):1558 – 1572, 2010.

[3] L. Demkowicz and J. Gopalakrishnan. A class of discontinuous petrov–galerkin methods. ii. optimal test functions. *Numerical Methods for Partial Differential Equations*, 27(1):70–105, 2011.